CFD Letters

Spiral Groove Bearing Geometry Variation Effect on Left Ventricular Assist Device Impeller Performance

Open Access

Shirly Empaling[1], Ahmad Zahran Md Khudzari[1,2,*], Muhammad Rashidi Abdul Kadir[1], Kahar Osman[1,2], Akmal Hakim Mohamad Hudzari[1], Mohammad Hasbullah Padzillah[3,4], Ishkrizat Abdul Talib[5], Mohamed Ezani Abdul Taib[6], Aizai Azan Abdul Rahim[6]

[1]   School of Biomedical Engineering and Health Sciences, Faculty of Engineering, Universiti Teknologi Malaysia, 81310 Skudai, Johor, Malaysia
[2]   IJN-UTM Cardiovascular Engineering Centre, Institute of Human Centered Engineering, Universiti Teknologi Malaysia, 81310 Skudai, Johor, Malaysia
[3]   School of Mechanical Engineering, Faculty of Engineering, Universiti Teknologi Malaysia, 81310 Skudai, Johor, Malaysia
[4]   UTM-Centre for Low Carbon Transport (Locartic), Institute of Vehicle System and Engineering, Universiti Teknologi Malaysia, 81310 Skudai, Johor, Malaysia
[5]   Faculty of Mechanical and Manufacturing, Universiti Tun Hussein Onn Malaysia, Parit Raja, Johor, Malaysia
[6]   Institut Jantung Negara, 50400, Kuala Lumpur, Malaysia

ARTICLE INFO	ABSTRACT
	Mechanical heart assist device has been accepted as a reliable treatment modality for advanced heart failure patient option other than orthotropic heart transplantation. One type of the device is a centrifugal rotary mechanical blood pump that has an impeller levitated using a magnetic motor system in which, it reduces blood damage compared to its predecessors. Spiral Groove Bearing (SGB) is proposed as another design consideration to further decrease blood damage, increasing blood flow in the tight gaps, while maintaining pump performances. There were few studies investigating several aspects of SGB effect on blood flow within the mechanical blood pump, however no study has been done on the SGB geometry configurations, and its effect on device performance. In this study, two design factors of SGB geometry were simulated using computational fluid dynamics (CFD) software – a gap between impeller and housing, and SGB groove depths. The resulting variants were then evaluated using several performance indexes which are pump pressure output, average washout flow, hemolysis index, bearing load carrying capacity and pump efficiency. From the results, there are two conclusions that can be drawn. By deepening SGB groove depth, blood pump performance increased, while increasing the gap between the impeller and pump housing, most performance indexes were reduced. Scoring and screening method was also utilized to evaluate the best variant and it was found that, the variant with SGB groove depths 1000 μm and gap of 80 μm was the best in term of overall performances.

---

* *Corresponding author.*
E-mail address: zahran.kl@utm.my (Ahmad Zahran Md Khudzari)

1. Introduction

Left Ventricular Assist Devices (LVADs) have been utilized for decades as one of the preferable auxiliary treatment for end-stage Heart Failure (HF) survivors. At present, 26 million people worldwide suffering from this life-threatening disease and about 5.7 million of new patients have been diagnosed with HF annually which makes HF to be one of the most pervasive and complicated medical condition [1][2]. The remarkable substitution of LVAD as an alternative treatment for heart transplant have shown an improvement on the patient survival rate up to 80% in the first year and 70% in the second year [3]. Although the successful outcome has been recorded, the ongoing researches have been continuously conducted in dealing with the major problem of producing the reliable and durable devices especially in countering complications such as blood haemolysis and thrombus formation in which it is mainly associated with the blood flow through the pump.

Non-contact bearing such as a magnetic levitation bearing system was introduced in the third generation of the blood pump in order to address the high rate of haemolysis occurrence [4]. One of the most likely region to occur is at the gap between the impeller shroud and pump housing in which the improper design configuration of the gap could increase the haemolysis and thrombus formation of the blood pump. Hence, to improve the blood flow in small pumps gap, spiral groove bearing (SGB) is proposed. SGB is a hydrodynamic bearing with logarithmic grooves engrave at the surface, acting as inferior impeller to drive the flow in pump gap. A stable blood film would be established within the narrow gap between the impeller and the pump lower housing once the rotary speed reaches a certain value of rotary speed according to the lubrication theory [5] . Hence, due to hydrostatic pressure generated, the impeller can be levitated passively and drives blood flow away to mitigate the thrombus formation inside the blood pump especially the region under the impeller.

 The implementation of spiral groove bearing (SGB) in the miniature blood pump was first introduced by Kink and Reul [6]. A study conducted by Kosaka *et al*. [7] proved that SGB in the centrifugal pump shows a low haemolysis occurrence and no evidence of thrombus formation. Additionally, Yamane et al. reported that, SGB reduces the thrombus formation in bearing gap by 3% of external flow in the pump [8]. Han et al. also came up with a novel pump out design that reduces of SGB width as radius increases resulting in good compromise with load carrying capacity and washout flow compared to the conventional design using computational fluid dynamic (CFD). The greatest contribution in SGB study marked by the Muijderman *et al*. in 1964 [9] when he derived equation for pressure distribution over the groove surfaces and bench top experiment was used for validation. However, inertia effect was neglected in his study because of air was used as the bearing medium. Muijderman finding although significant, is not applicable for blood due to significant differences in its viscosity and density. Chan et al., stated the results by Muijderman was over predicted and corrected it by presenting an improved design bearing displaying a good agreement between experiment and CFD simulation [10]. Amaral *et al*. [11] proved that SGB was able to reduce the residence time from 31 to 27ms (14% reduction) compared to the one without groove however, the study did not calculate the overall haemolysis index while varying depth that was cut from 50µm to 200µm.

In this study, investigation on selected design parameters was presented in viewing the performance and hemodynamic characteristics by implementation of SGB in blood pump. This simulation applies CFD method to investigate the effects of varying groove depth and bearing gap on the overall performance of the blood pump. It is hoped that the finding from this study will be beneficial for mechanical blood pump design in the future.

2. Methodology

2.1 Pump Geometrical Model and Computational Details

The pump geometries of this study was based on the proposed centrifugal rotary blood pump by A. Hilton [12], in which it emphasized the combination of existing standard industrial centrifugal blood pump designed by Karassik *et al*.[13], Lobanoff and Ross *et al*.[14] to the size of a LVAD. Three dimensional (3D) modelling software was used to design the blood pump with 7-bladed impeller with diameter of 44.8mm as shown in Figure 1 and the flow field was simulated with ANSYS. For the best mesh quality, the maximum mesh skewness of the model was ensured to be below 95 percent while the average skewness mostly as low as 0.22 was obtained. SST turbulence model is chosen for this study as it is proven to result in good agreement for flows through obstructed geometries either thru abrupt change in geometries [15] or narrow flow channels [16]. SST model has the advantage in simulating better flow separation and recirculation under adverse pressure gradient in comparison to other comparable model k-ε or k-ω [17]. The wall non-dimensionalized (y+) was considered for SST turbulence model and the value was ensured to be as close to 1 as possible for areas that are significant in this study such as impeller blade region and spiral groove profile while keeping the overall value close to 5. Grid independence test (GIT) was carried out to determine the appropriate size of mesh to be used wherein the pressure output and torque were used as a benchmark. Each pump was meshed using 1.53 million cells comprising of tetrahedral cells with 348K computational nodes for a complete pump assembly as shown in Figure 2.
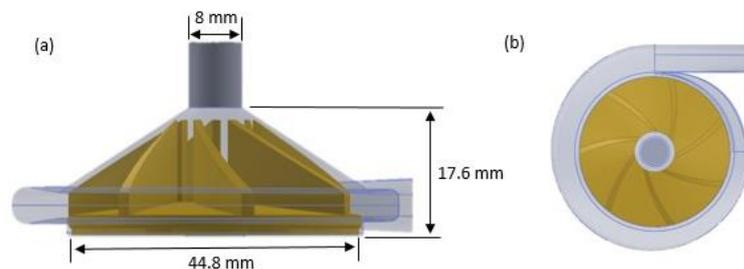
Fig. 1. (a) Side-view of the complete pump assembly (b) top-view of the geometry model of blood pump
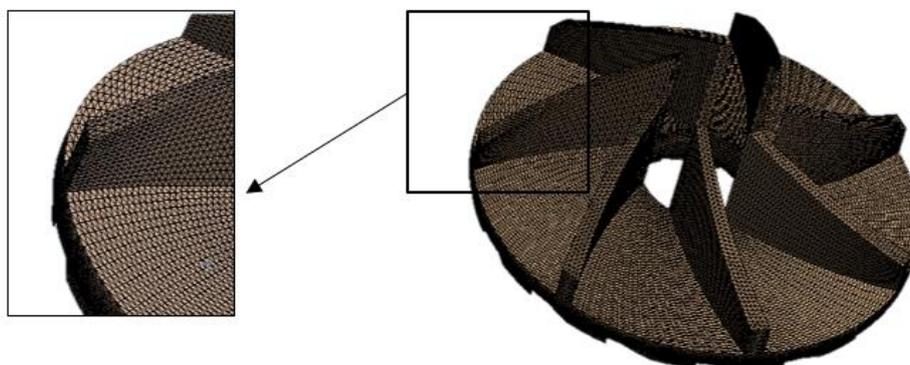
Fig. 2. Unstructured computational mesh of the pump impeller

Validation of the numerical simulation were carried out and compared to the experimental data by Das *et al.* [18] due to the similarity in diameter. A validation model was recreated to match the diameter and blade height of the design and the comparison is illustrated in Figure 3. At the studied flowrate of 5L/min, the pressure head differences between the validation model results and experimental data is only 6.71%, this shows a fairly good agreement suited for the present study.
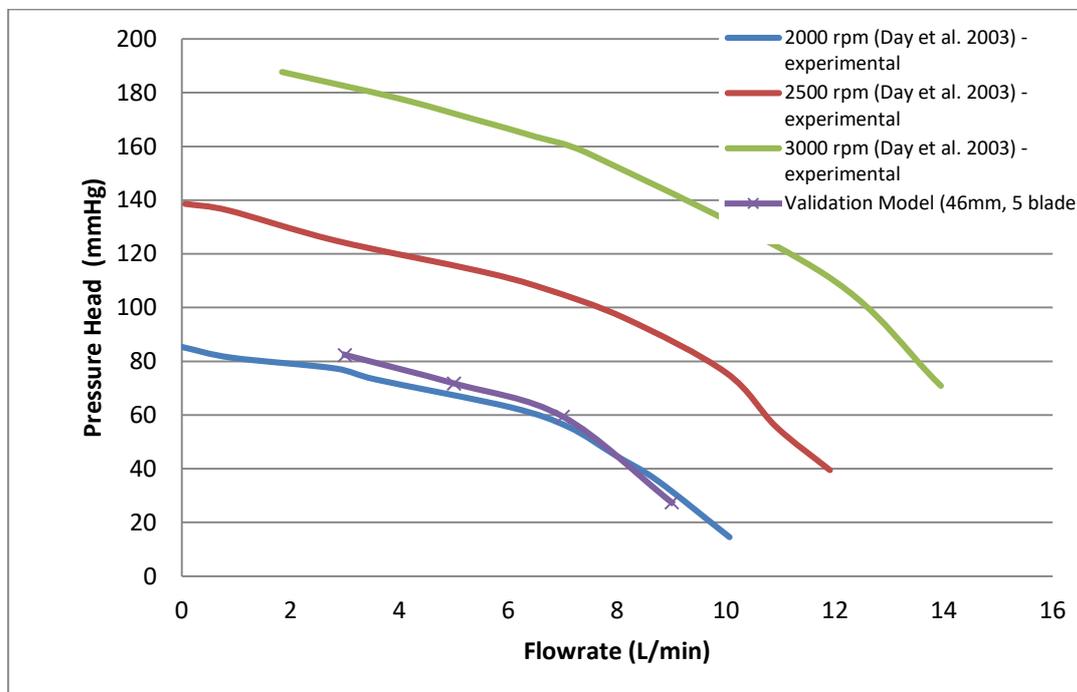
Fig. 3. Comparison of pressure head generated of current study with both numerical and experimental results by Das *et al.* [18]

In this numerical study, blood was treated as an incompressible Newtonian Fluid with viscosity and density; 0.0036 Pa.s and 1050kg/m^3 respectively. It is well known that blood particle to be non-Newtonian fluid, however for the present study, the blood is assumed to behave similarly as the Newtonian Fluid due to high shear stress in the rotary blood pump which is greater than 100s^{-1}. A constant angular speed of 2000 rpm was maintained with 5 L/min in order to support end stage of heart failure patient [19]. The model geometry was divided into three domains; the inflow, the impeller region (rotating region) and the volute region. Frozen rotor or multiple frames of reference (MRF) method was applied as interfaces between the rotational and stationary component. It is a steady state approximation in which cell zones can be assigned at different rotational speed and the grid remains fixed for the computation. The inlet pressure of 0 mmHg was used for all models which represents the pressure at left ventricle during diastole. Shear stress turbulence (SST) model was selected as it effectively blends the robustness, reasonable accuracy of formulation, wide flow ranges and computational economy. This model consist of kω model which considered to be more accurate for flow field prediction in near-wall region with freestream independence of the kε modelling in far field [20].

2.2 Proposed Spiral Groove Bearings

In this study, the blood pump used was a combination of the passive magnetic levitation system and hydrodynamic system of spiral groove design (as shown in Figure 4). To address the need for a

safe alternative bearing design while lowering pump power consumption and to improve blood flow in small pumps gaps, a spiral groove bearing (SGB) is proposed. The SGB is a hydrodynamics bearing with logarithmic grooves etched into the surface, acting as secondary impeller to drive the flow in secondary pumps gap. The bearing also provides stiffness by generating pressure as fluid travels along the narrowing grooves.
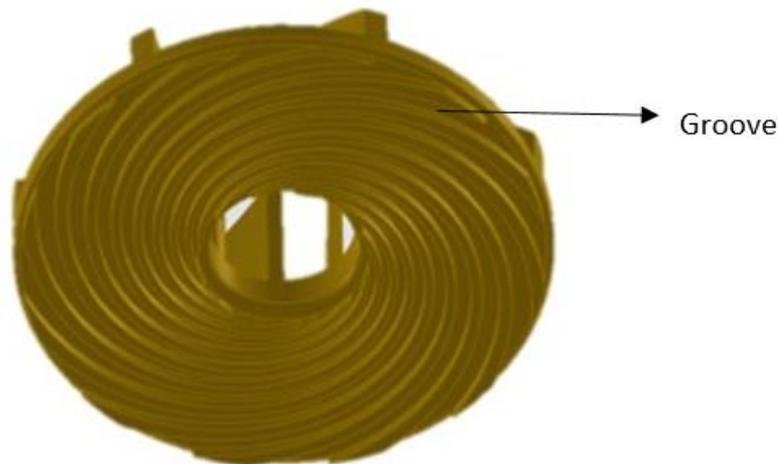
Fig. 4. Spiral groove profile at the bottom of the impeller

Table 1 outlines the geometric parameters of groove profile used in the study. The logarithmic spiral profile was drawn using Eq. 1 where the radius of the spiral groove is a function of the angular position around the rotational central axis of the bearing.

Table 1
Groove Profile Geometry Parameters

Component	Parameter	Value
Spiral Groove Bearing	Groove inner radius, r_{ig} (mm)	7.1
	Number of grooves, k	12
	Groove to ridge ratio	1

$$r(\theta) = r_{ig}e^{\theta tan\alpha} \tag{1}$$

Groove radius was calculated for selected angular position from 0 to 180 degrees. The groove radius is denoted by $r(\theta)$ in Eq. 1, r_{ig} is the initial radius of the groove profile, and α is the groove angle. The x and y coordinates of the outer radii were obtained from Eq. 3 and Eq. 4 while, Eq. 5 and Eq. 6 were used for inner radii. The inner radii were calculated with inclusion of an offset radius. This offset angle is calculated using Eq. 7. The groove to ridge ratio was taken as 1 which is the groove angle divided the ridge angle in which the width of SGB remained the same with increasing radius.

$$\alpha = \frac{\pi}{180} \times k \tag{2}$$

$$x_{(outer.groove)} = r\sin(\theta) \tag{3}$$

$$\gamma_{outer.groove} = r\cos(\theta) \tag{4}$$

$$x_{(inner.groove)} = r\sin(\theta + offset.angle) \tag{5}$$

$$\gamma_{(inner.groove)} = r\cos(\theta + offset.angle) \tag{6}$$

$$offset.angle = \frac{360}{[k+(k\times groove.to.ridge.ratio)]} \tag{7}$$

Key parameters (as illustrated in Figure 5) that were investigated in this study are the groove height, h_1 vs gap between impeller bottom and pump housing h_2 as shown in Table 2 below. These variations resulted in a total of six design variants. Parameter ranges were chosen based on literature and existing technology with novel or deeper groove depth. For the size of groove gap, we selected a lower bound of 80μm and an upper bound of 200μm based on the dimensions of smallest gap between impeller and housing of the HVAD and the HM3 (HeartMate 3, Abbott/ Thoratec) respectively [21].

Table 2
Investigated geometry parameter values

Component	Parameter	Value
Spiral Groove Bearing	Groove Depths, h_1 (μm)	500, 800, 1000
	Groove Gap, h_2 (μm)	80, 200
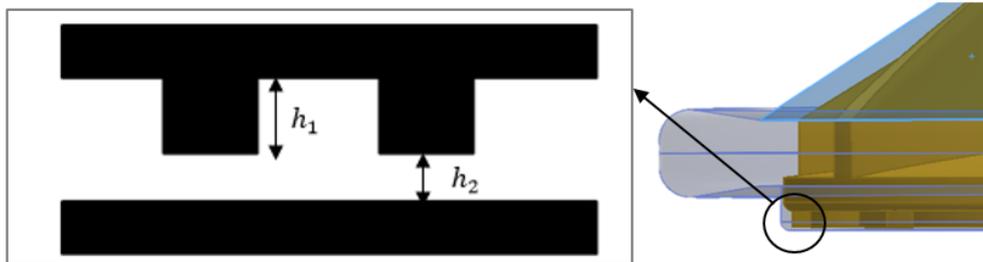
Fig. 5. Spiral groove bearing profile

2.3 Evaluation of Shear-Induced Haemolysis

Haemolysis or damage of erythrocytes occur mainly due to shear stress and time exposure to such shear stress. In this study, blood trauma was estimated by computing 6000 particles as the pump rotates at 2000 rpm speed. It is known as Langrangian particle tracking method in which the flow trajectories to estimate the haemolysis experience by the blood cell is calculated. Various methods were used to quantify the blood damage calculation in CFD but the most commonly used is the power law equation developed by Giersiepen *et al*. [22] shown in the Eq. 8.

$$BDI(\% = \frac{\Delta Hb}{Hb}(\%) = Ct^{\alpha}\tau^{\beta} \tag{8}$$

$BDI(\%)$ and $\frac{\Delta Hb}{Hb}(\%)$ quantifies the blood damage sustained by the blood cell, τ is the shear stress and t is the exposure time of that shear stress, while α, β and C are constant value. The limitation when applying these coefficients is that the constants value are-derived from uniform-shear experiments in Couette-type flow, to current problem. However, it was assumed that, this will not affect the comparative evaluation since the principle behind shear-stress induced effect on blood component are comparable to blood pump, an application that is seem reasonable. It was later proposed by Grigioni *et al.* [23] that summation of the individual contributions along a pathlines does not account for shear history of the red blood cells in which an already stressed cell membrane may be damaged more as the stress maintained. Different approach was then proposed that redefines the blood damage in term of mechanical dose, *D* function as:

$$D = t.\tau^{\frac{b}{a}} \tag{9}$$

Thus, the term is substituted into equation (Eq. 8)

$$\text{BDI} = C.D^a \tag{10}$$

The derivative of blood damage for time interval

$$D(t) - D(t_0) = \int_{t_0}^{t} \tau(\emptyset)^{\frac{b}{a}} d\emptyset \tag{11}$$

where $t = \tau(t)$ is a function of time and t_0 represents the starting point of observation. The value for one infinitesimal interval of blood damage can be estimated as

$$d(BDI) = d(CD^a) = C_a D^{a-1} dD \tag{12}$$

The blood damage index expressed as the integral sum of the infinitesimal contribution represented as

$$d(BDI) = [\int_1^N Ca \, [\tau(t_j)^{\frac{b}{a}} \, dt + D(t_0)]^{a-1} \tau(t_i)^{\frac{b}{a}} dt \tag{13}$$

In discrete form

$$d(BDI) = \sum_i^N Ca[\sum_{j=1}^i \tau(t)^{\frac{\beta}{a}} \Delta t]^{a-1} \tau(t_i)^{\beta/\alpha} \Delta t \tag{14}$$

where $\Delta(BDI)$ quantifies blood damage sustained by the blood cell in the ith interval, N is the number of observation time intervals along the fluid pathline, τ is a function of stress that varies with position along the pathline. The constants value of the equation used in this investigation of recent blood damage study that uses the constants proposed by Heuser et al.; α =1.991; β = 0.765; C = 0.0000018. The term in the bracket represents the mechanical dose moving along the pathline from the starting time until the ith instant, the weighted summation of Δt_j from t_0 to t_i. The blood damage index is then converted to Normalized Index of Hemolysis (NIH) to provide value of blood damage in the value of damage in the pump as shown in Eq. 15.

$$NIH = 100 \times \frac{\Delta Hb}{Hb} \times (1 - H_{ct}) \times k \tag{15}$$

where k is the haemoglobin content of blood. Typical values of H_{ct} and k are 45% and 150 g/L [24]. Blood trauma predictions were computed implementing the investigated formulations by means of a user-defined R code.

2.4 Mechanical Blood Pump Performance Index

The evaluation for the mechanical blood pump depends on several indexes. Those are pump pressure head output, pump efficiency, average washout flow, load carrying capacity, and haemolysis index. Pressure head output value is the pressure at the outlet of the pump, signifying the energy imparted to the blood coming into the aorta with existing pressure. Pump efficiency is the mechanical work of the impeller against the input energy by the pump, while average washout flow is the secondary flow between impeller bottom and pump housing. The load carrying capacity index is the amount of upward force theoretically generated by the thin film between the impeller and the pump housing. Haemolysis index as elaborated earlier is the level of damage on red blood cells within the mechanical blood pump.

2.5 Optimum Model Evaluation Method

With all performance indexes determined previously Design of Experiment (DoE) method was used to investigate different parameters effect on mechanical blood pump performance as per study done by Darlis et al for another type of medical device [25]. Using DoE method, two (2) design factors were selected: 1) gap between impeller bottom and housing (80 μm and 200 μm), and 2) SGB groove depth (500 μm, 800 μm, and 1000 μm), resulting into six variants (2 x 3 = 6) with varying degrees of gap and groove depth to achieve the objective of this study. It is also a pertinent matter to determine which variant exhibited the most optimum performance in all aspects. Selection method (tabulated in Table 3) with weightage approach is utilized, where each performance indexes was given a different numerical value as a weightage. The value for each indexes is depending on its perceived importance as a mechanical blood pump to support heart failure patient, rather than the pump mechanical performance. As such, haemolysis index is assigned the highest value at 35%, while pump pressure head output and pump efficiency is set at 10% each. This will inevitably bias any variants that has better performance as a pump for blood deliverance compared to just a good mechanical pump.

Table 3
Weightage for each performance index used in this study

Performance Index	Weightage (%)
Pressure Head Output	10
Pump Efficiency	10
Average Washout Flow	20
Load Carrying Capacity	25
Haemolysis Index	35

3. Results and Discussions

There are two different aspects provided in this section: pump performance factors and the evaluation method to determine which variants was the best among the six models.

3.1 Pump Performance

This section discusses the results obtained from the simulation work on the mechanical blood pump model. The effects of pressure head output, pump efficiency, average washout flow and haemolysis index are discussed in the next sub section.

3.1.1. Pressure head

Pump pressure head output is closely related to the pump performance. It was expected that the pump will yield 100 mmHg of pressure output so that the blood can be pushed into the aorta which has mean arterial pressure (MAP) of roughly 50 - 70 mmHg for heart failure patient. Table 4 illustrates the pressure output for the model variants. It can be seen that most of the variants were successful in delivering the desired pressure head output. The maximum pressure head output is 108.9 mmHg by combination of 80 μm and 1000 μm groove depth, while the variant with 80 μm and 500 μm showed the smallest pressure head output.

The effect of increasing groove depth from 500 μm to 1000 μm has resulting an increase of the pressure head output although the overall increment was not very distinctive which is by 6.28%. Similarly, to a lesser degree, the difference in the gap between impeller and pump housing also contributed to a small increment.

Table 4
Pump pressure head output [mmHg]

Groove Depth	Gap		
	80 μm	200 μm	Mean
500 μm	99.9	103.2	101.5
800 μm	104.9	105.9	105.4
1000 μm	108.9	107.7	108.3
Mean	104.6	105.6	
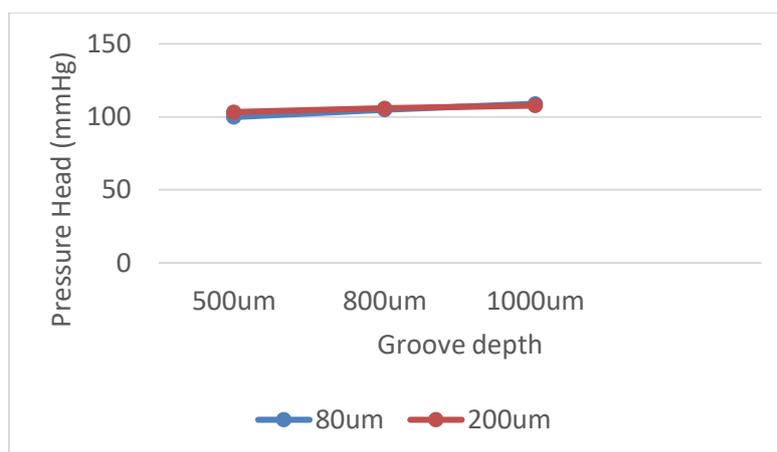
Fig. 6. Output Pressure for varying groove depth at rotating speed 2000 rpm outflow 5 L/min

From Figure 6, it can be seen that not much differences are evident with increasing gap between impeller bottom from the housing from both 80 μm and 200 μm, although at 1000 μm, both gap values are slightly higher. From these results, it can be concluded that the overall effect of varying gap and groove depth on pressure head output is minimal, although not an adverse effect for the

mechanical blood pump performance. All in all, the various configuration of the groove bearing in the gap would not affect in term pump performance as the driving force of the pump which are the impeller blades remains unchanged.

3.1.2. Efficiency

Pump efficiency is a measure of pump performance given to the input energy, and expanded energy. The formula for pump efficiency is the ratio between work of the shaft (in this case the impeller pressure multiplied by flow rate), and hydrodynamic power output as outlined in Eq. 16, where P is the pressure head, Q is the pump flow rate, T is the torque acting on the impeller at its axis, and ω is the blood pump rotational speed in rad/s.

$$\eta = \frac{PQ}{T\omega} \tag{16}$$

Table 5 shows the overall efficiency range of the model variants are below 60% in overall (range: 56.9 - 59.9%). Between varying bearing gap, there is no significant difference as the gap is increased from 80 μm to 200 μm with a similar mean value. There is a slight increase when the groove depth is increased from 500 μm to 1000 μm. Among the variants, the highest efficiency obtained is by variant with 80 μm bearing gap with 1000 μm groove depth.

Table 5
Mechanical blood pump efficiency

Groove Depth	Gap		
	80 μm	200 μm	Mean
500 μm	56.9	58.1	57.5
800 μm	57.8	57.9	57.8
1000 μm	58.2	58.6	59.2
Mean	58.2	58.2	

From Figure 7, it could be seen that not much differences are evident with increasing groove depth from both 80 μm and 200 μm across the increasing groove depth from 500 μm until 1000 μm (< 3%). The efficiency varies linearly with increasing groove depth and gap in this study may be as a result of volumetric losses from the washout flow. This much results suggested that as far as efficiency is concerned, by varying gap and groove depth, not much difference will be yielded, and thus may not be a high concern enough as long as there is enough external power for impeller rotation.

3.1.3. Washout flow

The washout flow is the secondary flow within the gap between the impeller and the pump housing. The higher the flow within the gap region, the better the washout feature of the model variant. Analysis of the washout flow shows that the flow rate increased with increased in pressure differences. In Table 6, the range of washout flow obtained for the model variants are from 0.018 mL/min until 0.046 mL/min, where the variant with 80 μm and groove depth of 500 μm has the lowest washout flow, while variant with gap 200 μm and 1000 μm yields the highest washout flow at 0.046 mL/min.
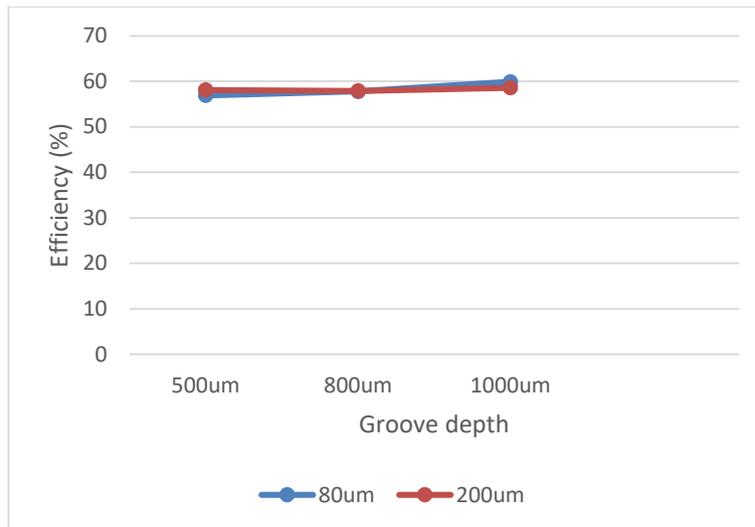
Fig. 7. The curve of efficiency against groove depth at rotating speed 2000 rpm outflow 5L/min

Table 6
Average washout flow (mL/min) between pump impeller and pump housing

Average Washout Flow (mL/min)	Gap		
Groove Depth	80 μm	200 μm	Mean
500 μm	0.018	0.033	0.026
800 μm	0.025	0.04	0.033
1000 μm	0.042	0.046	0.044
Mean	0.028	0.040	
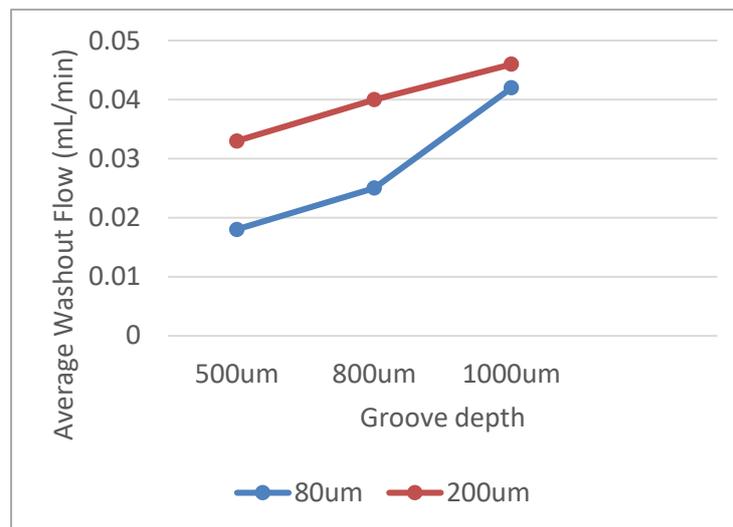
Fig. 8. Mean washout flow through the spiral groove bearing versus groove depth height at rotating speed 2000 rpm outflow 5 L/min

The effect of washout flow is apparent for both bearing gap and groove depth. At smaller bearing gap, the flow is evidently more restricted as compared to the larger gap variant which translate as

having lesser washout flow for smaller gap. Similar can be said for the groove depth, that larger groove depth would provide a deeper flow channel for better washout flow that increased to almost double the value from 80 μm to 200 μm bearing gap. Figure 8 shows mean washout flow through the spiral groove bearing versus groove depth height at rotating speed 2000 rpm outflow 5 L/min.

3.1.4. Load carrying capacity

The thin film between impeller and the housing also acts as a medium that separates between the two parts, providing passage for the blood from the centre of the pump into pump volute. The presence of the thin film also provides force on its own. In Table 7, the load carrying capacity results are tabulated. The minimum yield is from variant with 200 μm gap and 500 μm groove depth, while the biggest value is from variant with 80 μm gap, and groove depth of 1000 μm. With increasing groove depth, the mean value increased gradually, although the increment is not significant, while no much difference between gap groups as evidenced from the results (7.87 N vs 7.76 N). With the increasing washout flow in groove depth, the leakage would take away a lot of pressure energy of fluids in the grooves result in loss of the static pressure [26]. From here, it can be seen that load carrying capacity by varying gap and groove depth is not significant, and may have to be supplemented greatly with other means of impeller levitation and rotational push.

It can be seen that 80 μm has better load carrying capacity compare to 200μm gap. Thus, the tighter bearing gap has better load carrying capacity and loses load capacity as bearing gap widens. This is an expected trend as the load capacity is expected increases in a higher order behaviour as the film thickness decreases for a set groove height [12]. Figure 9 shows load carrying capacity versus groove depth height at rotating speed 2000 rpm outflow 5 L/min.

Table 7
Load carrying capacity for the six variants

	Gap		
Groove Depth	80 μm	200 μm	Mean
500 μm	7.61	7.34	7.48
800 μm	7.47	7.55	7.51
1000 μm	8.52	8.39	8.45
Mean	7.87	7.76	
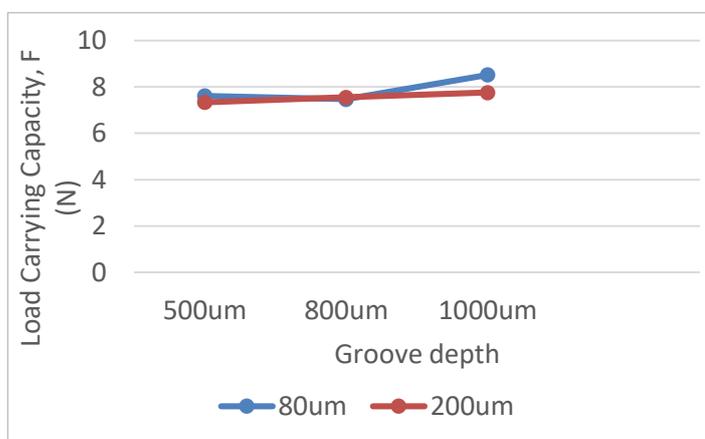
Fig. 9. Load carrying capacity versus groove depth height at rotating speed 2000 rpm outflow 5 L/min

3.1.5. Haemolysis index

Calculation of the haemolysis is obtained through Langrangian particle tracking. 6000 particles were inserted at the inlet of the pump and accumulation of stress was calculated to obtain haemolysis index as shown in Table 8. Figure 10 shows that the haemolysis index decrease with increasing groove depth. The same trend can be seen in gap between the impeller bottom and the housing. 80μm of gap between the impeller bottom and the housing the lowest haemolysis index due to smaller gaps lead to larger region of low speed [27]. The larger bearing gap results in larger washout flow. More flow travels through the gap resulting in higher haemolysis due more particles accumulating stress as they traverse the gap. As for groove depth however, the larger groove depth shows lower haemolysis. The lower haemolysis is apparent for large groove depth probably due to increase in low flow region as the deeper groove channel would result in low stress region of tracked particles traversing through this area.

Table 8
Haemolysis Index

Groove Depth	Gap		
	80 μm	200 μm	Mean
500 μm	0.026	0.048	0.037
800 μm	0.021	0.036	0.029
1000 μm	0.019	0.023	0.021
Mean	0.022	0.035	
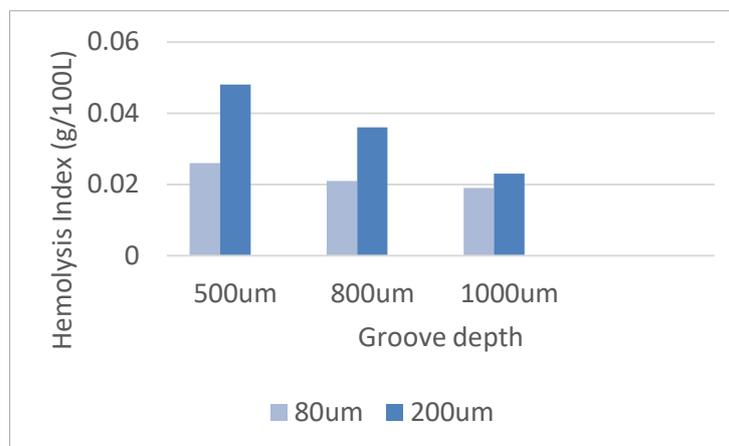
Fig. 10. Hemolysis Index comparison curve against groove depth at different groove gap between the impeller and housing

3.2 Evaluation for Optimum Model

All variants have yielded respective results, and to determine which variant is the most optimum, selection method is applied. In Table 9, each results are ranked according to increasing importance, i.e. the variant that is rank number one is the best in term of individual performance. For example, under the pump pressure head output, variants G8GD10 which is the simulation for pump model with gap of 80 μm and groove depth of 1000 μm is ranked number one (1) out of six variants. Similar exercise is carried out for all performance index, and the rank for each variants is summed up to yield overall rank.

Table 9
Variants results for each performance index and corresponding rank. G represents gap, while GH represents groove depth.

Variant	Pressure Output	Rank	Efficiency	Rank	Load Carrying Capacity	Rank	Average Washout Flow	Rank	Haemolysis Index	Rank	TOTAL	RANK
G8GD5	99.86	*6*	56.9	*6*	7.613	3	0.018	*6*	0.0255	*4*	25	*6*
G8GD8	104.93	*4*	57.8	*5*	7.466	5	0.025	*5*	0.0211	*2*	21	*4*
G8GD10	108.91	*1*	59.9	*1*	8.516	1	0.042	*2*	0.0187	*1*	6	*1*
G20GD5	103.22	*5*	58.1	*3*	7.339	6	0.033	*4*	0.0476	*6*	24	*5*
G20GD8	105.85	*3*	57.9	*4*	7.545	4	0.04	*3*	0.0359	*5*	19	*3*
G20GD10	107.73	*2*	58.6	*2*	8.385	2	0.046	*1*	0.0229	*3*	10	*2*

The overall rank in Table 10 shows that variant G8GD10 is the best model variant out of six variants, contributed from several performance indexes where the rank is either number one or two resulting into an aggregate rank of six. This accumulative result is consistent with the previous subsection findings. The number one and two rank is from the same groove depth (1000 µm). The worse rank variant is G8GD5, followed by the second worse is G20GD5. These two results suggested at this moment that rather than the gap between impeller, it is groove depth that will contributed more to the mechanical blood pump performance.

Table 10
Variants results is ranked according to weightage predetermined

Weightage	10%	10%	25%	20%	35%	100%	
Variant	Pressure Head Output Rank	Efficiency Rank	Load Carrying Capacity Rank	Average Washout Flow Rank	Hemolysis Index Rank	TOTAL	FINAL RANK
G8GD5	0.6	0.6	0.75	1.2	1.4	4.55	*5*
G8GD8	0.4	0.5	1.25	1	0.7	3.85	*3*
G8GD10	0.1	0.1	0.25	0.4	0.35	1.2	*1*
G20GD5	0.5	0.3	1.5	0.8	2.1	5.2	*6*
G20GD8	0.3	0.4	1	0.6	1.75	4.05	*4*
G20GD10	0.2	0.2	0.5	0.2	1.05	2.15	*2*

4. Conclusions

In this study, the effect of groove profile variation on mechanical blood pump performance was evaluated in-silico. The investigation was conducted by applying Computational Fluid Dynamic (CFD) approach to simulate the natural behaviour of blood pump where in the occurrence of haemolysis event contributing the most in this study. The simulation results show a good compromise with the literature provided by previous researchers. Referring to the scoring method analysis, the variation of groove profiles coming from the group of 1000 µm groove depth were ranked in the first and second places. Groove depth of 1000 µm enhanced the hemocompatibility with 40-60% closest to 0.01g/100L of ideal benchmark of the haemolysis index. Moreover, inclusion of deeper spiral groove bearing display a higher washout > 0.042 mL/min at the gap enable the fluid to be driven to the main flow pathway thus prevent the thrombosis formation between the gap. Therefore, despite of varying the gap between bottom of the impeller and housing, groove depth shows a significance in term of

the result. Thus deeper groove increases the pump performance in this study. These findings enable improvement in term reducing blood damage as well as volumetric efficiency of the centrifugal pump.

Acknowledgement

References

[1]   Ponikowski, Piotr, Stefan D. Anker, Khalid F. AlHabib, Martin R. Cowie, Thomas L. Force, Shengshou Hu, Tiny Jaarsma et al. "Heart failure: preventing disease and death worldwide." *ESC Heart Failure* 1, no. 1 (2014): 4-25.

[2]   MEMBERS, WRITING GROUP, Emelia J. Benjamin, Michael J. Blaha, Stephanie E. Chiuve, Mary Cushman, Sandeep R. Das, Rajat Deo et al. "Heart disease and stroke statistics—2017 update: a report from the American Heart Association." *Circulation* 135, no. 10 (2017): e146.

[3]   Kirklin, James K., Francis D. Pagani, Robert L. Kormos, Lynne W. Stevenson, Elizabeth D. Blume, Susan L. Myers, Marissa A. Miller, J. Timothy Baldwin, James B. Young, and David C. Naftel. "Eighth annual INTERMACS report: special focus on framing the impact of adverse events." *The Journal of Heart and Lung Transplantation* 36, no. 10 (2017): 1080-1086.

[4]   Hoshi, Hideo, Tadahiko Shinshi, and Setsuo Takatani. "Third-generation blood pumps with mechanical noncontact magnetic bearings." *Artificial organs* 30, no. 5 (2006): 324-338.

[5]   Han, Qing, Jun Zou, Xiaodong Ruan, Xin Fu, and Huayong Yang. "A novel design of spiral groove bearing in a hydrodynamically levitated centrifugal rotary blood pump." *Artificial organs* 36, no. 8 (2012): 739-746.

[6]   Kink, Thomas, and Helmut Reul. "Concept for a new hydrodynamic blood bearing for miniature blood pumps." *Artificial organs* 28, no. 10 (2004): 916-920.

[7]   Kosaka, Ryo, Kazuya Yasui, Masahiro Nishida, Yasuo Kawaguchi, Osamu Maruyama, and Takashi Yamane. "Optimal bearing gap of a multiarc radial bearing in a hydrodynamically levitated centrifugal blood pump for the reduction of hemolysis." *Artificial organs* 38, no. 9 (2014): 818-822.

[8]   Yamane, Takashi, Osamu Maruyama, Masahiro Nishida, Ryo Kosaka, Daisuke Sugiyama, Yusuke Miyamoto, Hiroshi Kawamura et al. "Hemocompatibility of a hydrodynamic levitation centrifugal blood pump." *Journal of Artificial Organs*10, no. 2 (2007): 71-76.

[9]   Muijderman, E. A. "Analysis and design of spiral-groove bearings." *Journal of Lubrication Technology* 89, no. 3 (1967): 291-305.

[10]   Chan, Weng-Kong, Kim-Tiow Ooi, and Yan-Chuan Loh. "Numerical and in vitro investigations of pressure rise in a new hydrodynamic blood bearing." *Artificial organs* 31, no. 6 (2007): 434-440.

[11]   Amaral, Felipe, Sascha Groß-Hardt, Daniel Timms, Christina Egger, Ulrich Steinseifer, and Thomas Schmitz-Rode. "The spiral groove bearing as a mechanism for enhancing the secondary flow in a centrifugal rotary blood pump." *Artificial organs* 37, no. 10 (2013): 866-874.

[12]   Hilton, Andrew. "Proposal for a cost-effective centrifugal rotary blood pump: design of a hybrid magnetic/hydrodynamic bearing." PhD diss., University of Nottingham, 2010.

[13]   Karassik, Igor J., Joseph P. Messina, Paul Cooper, and Charles C. Heald. *Pump handbook*. Vol. 3. New York: McGraw-Hill, 2001.

[14]   Lobanoff, Val S., and Robert R. Ross. *Centrifugal pumps: design and application*. Elsevier, 2013.

[15]   Jehad, D. G., G. A. Hashim, A. K. Zarzoor, and CS Nor Azwadi. "Numerical Study of Turbulent Flow over Backward-Facing Step with Different Turbulence Models." *Journal of Advanced Research Design* 4, no. 1 (2015): 20-27.

[16]   Jamil, M. M., M. I. Adamu, T. R. Ibrahim, and G. A. Hashim. "Numerical Study of Separation Length of Flow through Rectangular Channel with Baffle Plates." *Journal of Advanced Research Design Vol* 7, no. 1 (2015): 19-33.

[17]   Andersson, Bengt, Ronnie Andersson, Love Håkansson, Mikael Mortensen, Rahman Sudiyo, and Berend Van Wachem. *Computational fluid dynamics for engineers*. Cambridge University Press, 2011.

[18]   Hamed, A., D. Basu, and K. Das. "Effect of Reynolds number on the unsteady flow and acoustic fields of supersonic cavity." In *ASME/JSME 2003 4th Joint Fluids Summer Engineering Conference*, pp. 1049-1054. American Society of Mechanical Engineers, 2003.

[19]   Behbahani, Mehdi, M. Behr, M. Hormes, U. Steinseifer, D. Arora, O. Coronado, and M. Pasquali. "A review of computational fluid dynamics analysis of blood pumps." *European Journal of Applied Mathematics* 20, no. 4 (2009): 363-397.

[20] R. Just, "a Mechanism Design Approach," *Agric. Econ.*, vol. 82, no. February, pp. 14–24, 2000.

[21] Schmitto, Jan D., Jasmin S. Hanke, Sebastian V. Rojas, Murat Avsar, and Axel Haverich. "First implantation in man of a new magnetically levitated left ventricular assist device (HeartMate III)." *The Journal of Heart and Lung Transplantation* 34, no. 6 (2015): 858-860.

[22] Giersiepen, M., L. J. Wurzinger, R. Opitz, and H. Reul. "Estimation of shear stress-related blood damage in heart valve prostheses-in vitro comparison of 25 aortic valves." *The International journal of artificial organs* 13, no. 5 (1990): 300-306.

[23] Grigioni, Mauro, Umberto Morbiducci, Giuseppe D'Avenio, Giacomo Di Benedetto, and Costantino Del Gaudio. "A novel formulation for blood trauma prediction by a modified power-law mathematical model." *Biomechanics and Modeling in Mechanobiology* 4, no. 4 (2005): 249-260.

[24] Carswell, Dave, Andy Hilton, Chris Chan, Diane McBride, Nick Croft, Avril Slone, Mark Cross, and Graham Foster. "Development of a radial ventricular assist device using numerical predictions and experimental haemolysis." *Medical engineering & physics* 35, no. 8 (2013): 1197-1203.

[25] Darlis, Nofrizalidris, Kahar Osman, Muhamad Hasbullah Padzillah, Jeswant Dillon, and Ahmad Zahran Md Khudzari. "Modification of Aortic Cannula With an Inlet Chamber to Induce Spiral Flow and Improve Outlet Flow." *Artificial organs* 42, no. 5 (2018): 493-499.

[26] Han, Qing, Jun Zou, Xiaodong Ruan, Xin Fu, and Huayong Yang. "A novel design of spiral groove bearing in a hydrodynamically levitated centrifugal rotary blood pump." A*rtificial organs* 36, no. 8 (2012): 739-746.

[27] Wiegmann, L., Stefan Boës, Diane de Zélicourt, Bente Thamsen, M. Schmid Daners, Mirko Meboldt, and V. Kurtcuoglu. "Blood pump design variations and their influence on hydraulic performance and indicators of hemocompatibility." *Annals of biomedical engineering* 46, no. 3 (2018): 417-428.